


Infusion of Human Mesenchymal Stem Cells Improves Regenerative Niche in Thioacetamide-Injured Mouse Liver

Ying-Hsien Kao¹ · Yu-Chun Lin² · Po-Huang Lee^{2,3} · Chia-Wei Lin⁴ ·
Po-Han Chen¹ · Tzong-Shyuan Tai¹ · Yo-Chen Chang⁴ · Ming-Huei Chou^{5,6} ·
Chih-Yang Chang⁷ · Cheuk-Kwan Sun^{1,8} 

Received: 9 April 2020 / Revised: 13 May 2020 / Accepted: 14 May 2020 / Published online: 3 September 2020
© The Korean Tissue Engineering and Regenerative Medicine Society 2020

Abstract

BACKGROUND: This study investigated whether xenotransplantation of human Wharton's jelly-derived mesenchymal stem cells (WJ-MSCs) reduces thioacetamide (TAA)-induced mouse liver fibrosis and the underlying molecular mechanism.

METHODS: Recipient NOD/SCID mice were injected intraperitoneally with TAA twice weekly for 6 weeks before initial administration of WJ-MSCs. Expression of regenerative and pro-fibrogenic markers in mouse fibrotic livers were monitored post cytotherapy. A hepatic stellate cell line HSC-T6 and isolated WJ-MSCs were used for in vitro adhesion, migration and mechanistic studies.

RESULTS: WJ-MSCs were isolated from human umbilical cords by an explant method and characterized by flow cytometry. A single infusion of WJ-MSCs to TAA-treated mice significantly reduced collagen deposition and ameliorated liver fibrosis after 2-week therapy. In addition to enhanced expression of hepatic regenerative factor, hepatocyte growth factor, and PCNA proliferative marker, WJ-MSC therapy significantly blunted pro-fibrogenic signals, including Smad2, RhoA, ERK. Intriguingly, reduction of plasma fibronectin (pFN) in fibrotic livers was noted in MSC-treated mice. In vitro studies further demonstrated that suspending MSCs triggered pFN degradation, soluble pFN conversely retarded adhesion of suspending MSCs onto type I collagen-coated surface, whereas pFN coating enhanced WJ-MSC migration across mimicked wound bed. Moreover, pretreatment with soluble pFN and conditioned medium from MSCs with pFN strikingly attenuated the response of HSC-T6 cells to TGF- β 1-stimulation in Smad2 phosphorylation and RhoA upregulation.

CONCLUSION: These findings suggest that cytotherapy using WJ-MSCs may modulate hepatic pFN deposition for a better regenerative niche in the fibrotic livers and may constitute a useful anti-fibrogenic intervention in chronic liver diseases.

Keywords Human umbilical cord · Hepatotoxin · Liver fibrosis · Plasma fibronectin · Wharton's jelly tissue

Ying-Hsien Kao and Yu-Chun Lin have contributed equally to this work.

Electronic supplementary material The online version of this article (<https://doi.org/10.1007/s13770-020-00274-4>) contains supplementary material, which is available to authorized users.

✉ Chih-Yang Chang
kentyan.chang@msa.hinet.net

✉ Cheuk-Kwan Sun
lawrence.c.k.sun@gmail.com

¹ Department of Medical Research, E-Da Hospital, No. 1, Yida Rd., Yanchau District, Kaohsiung 82445, Taiwan

² Department of Surgery, E-Da Hospital, Kaohsiung, Taiwan

³ Committee for Integration and Promotion of Advanced Medicine and Biotechnology, E-Da Healthcare Group, Kaohsiung, Taiwan

⁴ Department of Ophthalmology, Kaohsiung Medical University, Kaohsiung, Taiwan

1 Introduction

Liver fibrosis, which is characterized by an excessive deposition of extracellular matrix (ECM) proteins, is considered to be a wound-healing response to a variety of chronic stimuli [1, 2]. Following liver injury, pro-inflammatory cytokines initiate the wound healing processes including liver regeneration orchestrated by various molecular and cellular participants. Meanwhile, the upregulated expression of hepatic transforming growth factor- β 1 (TGF- β 1) potently activates hepatic stellate cells (HSCs), which is the primary cell type in the liver undergoing myofibroblastic phenotype transformation in response to hepatic insult but is also responsible for excessive ECM production in fibrotic livers, in particular collagen fibrils [2, 3]. The TGF- β 1-driven profibrogenic signaling is well known to be delivered through the canonical Smad pathway [2, 3]. Besides, TGF- β 1 induces the activation of extracellular signal-regulated kinase 1/2 (ERK1/2) [4] and the protein expression of Ras homolog gene family member A (RhoA) that activate HSCs via a Smad-dependent mechanism [5].

Mesenchymal stem cells (MSCs) are found to reside in diverse adult tissues and have been claimed to be therapeutic against a broad range of human diseases currently refractory to conventional treatments. Adult MSCs have been identified in various organs including bone marrow (BM), brain, liver, skeletal muscle, and umbilical cord [6]. Wharton's jelly of the umbilical cord is a potential source for MSC isolation. Because Wharton's jelly-derived MSCs (WJ-MSCs) show fibroblast-like morphology [7], they were once considered to be myofibroblasts [8, 9]. Ex vivo studies have demonstrated the capacities of WJ-MSCs for differentiating into different cell lineages, including adipocytes [10], osteocytes [10], chondrocytes [11], neurons [12], islet-like cells [13], myocytes [14], and endothelial cells [15], illustrating their therapeutic potential against a variety of diseases in different organs. Recent in vitro and in vivo findings have also indicated that WJ-MSCs, after hepatogenic induction, could differentiate into hepatocyte-like cells expressing hepatocytic markers including albumin, α -fetoprotein and cytokeratin 18 [16, 17] and that WJ-

MSCs administration could improve experimental liver fibrosis and regeneration in rats [18, 19]. All evidence suggests that WJ-MSCs may be promising for tissue engineering and cell therapy against chronic liver diseases.

Sakaida et al. were the first to demonstrate the therapeutic potential of BM-derived MSCs against carbon tetrachloride (CCl₄)-induced liver fibrosis in a murine model [20]. Studies later showed that the upregulation of matrix metalloproteinases (MMPs) in the implanted cells is responsible for ECM degradation and fibrosis resolution in the liver [21]. We previously found that infusion of BM stromal cells enhances liver regeneration and reduces fibrosis in the regenerating fibrotic rat livers [22]. Paradoxically, transplantation of UCB-derived CD34+ hematopoietic stem cells did not engraft in thioacetamide (TAA)-induced cirrhotic livers of rats [23], while administration of MSC-conditioned medium exerts similar anti-inflammatory and anti-fibrotic effects in CCl₄-injured mouse livers [24], suggesting that paracrine actions of stem cells may participate in liver regeneration. Although WJ-MSCs have been previously demonstrated to improve rat liver fibrosis induced by either CCl₄ [18] or TAA [19], the mechanism underlying the therapeutic potential of MSC has not been sufficiently addressed. This study, therefore, aimed at evaluating the therapeutic efficiency of human WJ-MSC xenotransplantation in the NOD-SCID mice with TAA-induced liver fibrosis, and further elucidating the underlying mechanism of MSC therapy against liver fibrosis.

2 Materials and methods

2.1 Isolation and characterization of WJ-MSCs

Protocol for collection of human umbilical cord was approved by Institutional Reviewing Board of our institute (EMRP26100N). WJ-MSCs were isolated from WJ tissues using a previously reported explant method [25]. The isolated WJ-MSCs were expanded in Iscove modified Dulbecco medium (IMDM; Invitrogen, Grand Island, NY, USA) containing 10% (v/v) FBS, 10 ng/mL bFGF (PeproTech, Rocky Hill, NJ, USA), 100 U penicillin, 1000 U streptomycin, and 2 mM L-glutamine (Invitrogen) and incubated at 37 °C in an incubator with 5% CO₂ at saturated humidity. Medium changes were carried out twice weekly and the cells were passaged with TrypLE™ Express enzyme (Gibco/Thermo Fisher, Grand Island, NY, USA), washed twice with PBS, centrifuged at 1000 rpm for 5 min, and replated at a ratio of 1:3 under the same culture conditions. Using flow cytometry, WJ-MSCs at passage 2 were phenotypically characterized with antibodies for MSC-expressing markers, CD44, CD73, CD90 and CD105,

⁵ Graduate Institute of Clinical Medical Sciences, Chang Gung University College Medicine, Kaohsiung, Taiwan

⁶ Center for General Education, Cheng-Shiu University, Kaohsiung, Taiwan

⁷ Department of Gynecology and Obstetrics, E-Da Hospital, I-Shou University, No. 1, Yida Rd., Yanchau District, Kaohsiung 82445, Taiwan

⁸ The School of Medicine for International Students, I-Shou University, Kaohsiung, Taiwan

as well as a cocktail of CD45/CD34/CD11b/CD19/HLA-DR antibodies for negative expression included in a commercially available kit for human MSC analysis (Stemflow™, BD Biosciences, San Jose, CA, USA). The percentages of CD marker expression were measured in a flow cytometer (Accuri™, BD Biosciences) with initial gating to exclude dead cells and debris. To confirm the *in vitro* differentiation potentials of the isolated WJ-MSCs, the expanded cells at passage 2 were grown with induction media for adipogenesis, osteogenesis and chondrogenesis before being subject to Oil red O, alizarin red S staining and pellete formation assays, respectively, for identification after the indicated periods of induction according to the methods previously described [26].

2.2 Quantitative polymerase chain reaction (qPCR) for differentiation markers

Total RNA was extracted from liver tissues and cultured cells using Trizol solution (Invitrogen, Gaithersburg, MD, USA). Reverse transcription and qPCR were performed as previously described. The primer sequences for detecting differentiation markers were listed in Supplemental Table 1.

2.3 Animal liver fibrosis induction

All animal experimental procedures, which were approved by and under surveillance of the Institute of Animal Care and Use Committee at our institute (Affidavit of Approval of Animal Use Protocol No. IACUC-101017), were performed in accordance with the Guide for the Care and Use of Laboratory Animals (NIH Publication No. 85-23, National Academy Press, Washington, DC, USA, revised 1996). Six-week-old male NOD-SCID mice were purchased from BioLasco Inc., and bred at 20–22 °C with 12 h light–dark cycle and free access to feed and water at an accredited animal facility. Chronic liver fibrosis was induced through intraperitoneal injection of TAA (200 mg/kg, Sigma-Aldrich Corporation, St. Louis, MO, USA) twice weekly for 6 consecutive weeks. Age-matched mice receiving saline only served as vehicle control.

2.4 MSC administration

Before cell administration, cultured adherent MSCs were rinsed with D-PBS and suspended at 1×10^6 cells/mL and labeled with 5 μM of Vybrant® CM-DiI (Molecular Probe, Eugene, OR, USA) for 5 min at 37 °C and then for an additional 15 min at 4 °C. Incubation at lower temperature allows the dye to label the plasma membrane instead of undergoing endocytosis, thereby minimizing dyeing of cytoplasmic vesicles. After washes with PBS, the labeled

MSCs were resuspended in fresh medium without serum and aliquoted into parts (3×10^5 cells suspended in 200 μL PBS). Cytotherapy was conducted in mice receiving 6 weeks of TAA treatment by injecting 3×10^5 WJ-MSCs suspended in PBS through the tail vein. The mice were sacrificed at 3, 7, and 14 days after initiation of cell therapy. At the end of the experiment, 1 mL of whole blood was collected by heart puncture under deep anesthesia, placed into heparinized tubes (Vacutainer, BD Diagnostics, Oxford, UK), and subject to biochemical analysis. After euthanasia of the animals, the liver, spleen, kidneys, and lungs were dissected and divided into two portions before being frozen at –80 °C for histological and molecular analyses, respectively.

2.5 Biochemistry

Mouse sera were thawed on ice and subject to biochemical quantifications, including aspartate aminotransferase (AST), alanine aminotransferase (ALT), alkaline phosphatase (ALP), blood urea nitrogen (BUN), uric acid (UA), and ammonia, using a clinical automatic analyzer.

2.6 Sirius red staining and histomorphometry

Sirius red staining was performed on formalin-fixed paraffin-embedded sections as previously described [27–29]. In brief, the rehydrated paraffin sections were stained in 0.1% Sirius red (Direct Red 80, Sigma) in saturated picric acid solution for 1 h, followed by washes with 0.5% acetic acid. Morphology of collagen fibers was documented with a light microscope (Olympus Optical Company, Tokyo, Japan). The area of collagen deposition was morphometrically measured using Image-Pro Plus software (Media Cybernetics, Bethesda, MD, USA) and at least five randomly captured low-power images in each section were counted. The percentages of collagen deposition area were calculated with the function of collagenous area divided by total image area.

2.7 Western blotting

Total protein of mouse livers or cultured cells were lysed in RIPA buffer containing protease inhibitor cocktail (Roche, Indianapolis, IN, USA) and quantitatively determined by using Coomassie protein assay kit (Pierce Biotechnology, Rockford, IL, USA). SDS-PAGE and Western blotting were performed as previously described [27]. The detecting antibodies including those against β-actin, hepatocyte growth factor (HGF), proliferative cell nuclear antigen (PCNA), and plasma FN (pFN) were from Abcam (Cambridge, MA). Anti-Ets-1, Smad2, p-Smad2, RhoA, ERK1/2

and p-ERK1/2 antibodies were purchased from Cell Signalling (Danvers, MA, USA).

2.8 Cell culture and in vitro assays

WJ-MSCs cultivated between passages 3 through 5 were used for cell adhesion and wound closure migration assays. Culture wares were pre-coated with 10 µg/mL of either pFN (Sigma) or type I collage protein extracted from rat tail tendons using a previous protocol [30]. Coating and assay procedures were performed as previously described [31]. The conditioned media from WJ-MSCs were collected after cultivation under serum-free condition for 24 h. An active form of HSC cell line, HSC-T6, was maintained as previously described [32] and used for TGF-β stimulation study.

2.9 Statistic analysis

In vivo and in vitro data are presented as mean ± standard error of the mean (SEM) and mean ± standard deviation (SD), respectively. Difference among groups was statistically analyzed by one-way ANOVA, followed by Bonferroni post hoc test for multiple comparisons. Significance is declared when *P* value is less than 0.05.

3 Results

3.1 Human WJ-MSC characterization

Primary MSCs migrated from umbilical cord explant tissues showed typical mesenchymal morphology and a rapid rate of proliferation for early passages (Fig. 1A, B). The explanted WJ-MSCs at passage 2 were characterized by expression of MSC-specific surface CD marker. Consistent with the finding of our previous study [26], flow cytometry showed the expressions of MSC phenotype markers, including CD44, CD73, CD90, and CD105, but not those of CD45/CD34/CD11b/CD19/HLA-DR surface antigens on WJ-MSCs (Fig. 1C). The multi-lineage differentiation potentials of isolated WJ-MSCs were further morphologically and transcriptionally investigated, including lipogenesis, chondrogenesis, and osteogenesis. Oil red O staining (Fig. 1D) and the expression profiles of PPAR-γ and GLUT4 genes by qPCR (Fig. 1E) indicated differentiation of WJ-MSC into lipocyte-like cells. Positive Alizard red staining (Fig. 1F) and upregulation of osteopontin and ALP genes (Fig. 1G) supported their osteogenic differentiating capacity. In addition, pellet formation assay (Fig. 1H) and induction of perlecan and syndecan genes (Fig. 1I) revealed the chondrogenesis capacity of the isolated WJ-MSCs.

3.2 WJ-MSC therapy ameliorated TAA-induced mouse liver fibrosis

To explore the therapeutic effect of the isolated WJ-MSCs on the hepatotoxin-injured liver, the cells were intravenously administered into the tail veins of mice that already received TAA for six consecutive weeks. At 3, 7 and 14 days post WJ-MSC administration, plasma samples of the mice were collected and subject to biochemistry analysis. Biochemistry measurement data indicated that, despite no differences in body weight and blood AST and ALT levels, MSC administration significantly reduced BUN levels after 3-day treatment and ameliorated UA and ammonia concentrations after 2 weeks of cell therapy (Supplemental Table 2). Although both PCR monitoring of human CK-18 gene and immunofluorescent visualization of labeled MSCs in the fibrotic livers revealed no implantation of administered WJ-MSCs in all treated mice (data not shown), histological observation following Sirius red staining (Fig. 2A) and subsequent morphometrical analysis (Fig. 2B) demonstrated that a single dose of WJ-MSC transiently increased intrahepatic collagen abundance in injured mouse livers at the early phase of therapy (i.e., 3 days post-treatment), while it significantly ameliorated collagen deposition in the livers after 2 weeks of treatment. The finding, therefore, suggested that WJ-MSC therapy improved regeneration of the injured mouse livers.

3.3 WJ-MSC therapy enhanced hepatic regeneration and reduced profibrogenic signals in mouse liver

To scrutinize the molecular mechanisms underlying the beneficial effects of MSC treatment, liver protein extracts were subject to western blotting analysis (Fig. 3A). The subsequent densitometry clearly showed that WJ-MSC injection increased hepatic abundance of HGF protein (Fig. 3B) and proliferative marker PCNA (Fig. 3C). Besides, WJ-MSC therapy significantly increased hepatic expression of Ets-1 p42 protein at least within 7 days of cell therapy (Fig. 3D). Because transcription factor Ets-1 is an oncogene responsible for hepatocyte proliferation [33], these findings strongly supported the enhancing effect of WJ-MSC treatment on liver regeneration. Densitometry analysis demonstrated that WJ-MSC treatment dramatically suppressed constitutive expression of Smad2 protein (Fig. 3E), which plays a pivotal role in conveying TGF-β1-mediated profibrogenic signal. Similar to its suppressive effect on Smad2 expression, WJ-MSC therapy after 7 days significantly reduced the expression of total RhoA protein that crucially contributes to liver fibrosis (Fig. 3F), and completely abrogated the early increase of ERK1/2 levels in TAA-injured mouse livers (Fig. 3G). Despite no

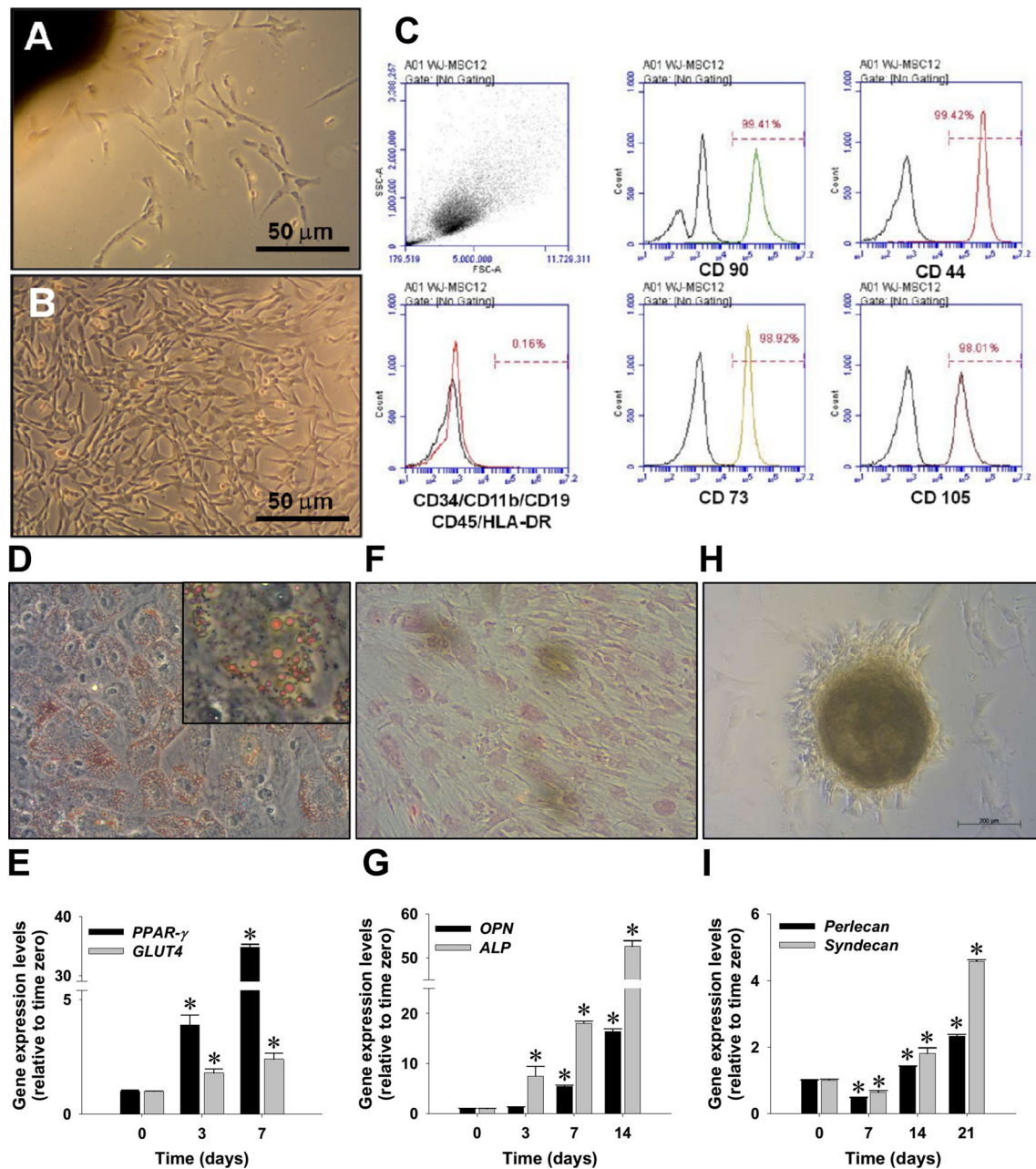


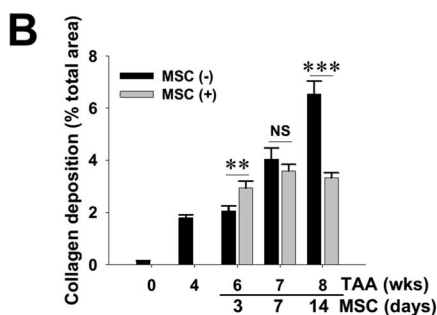
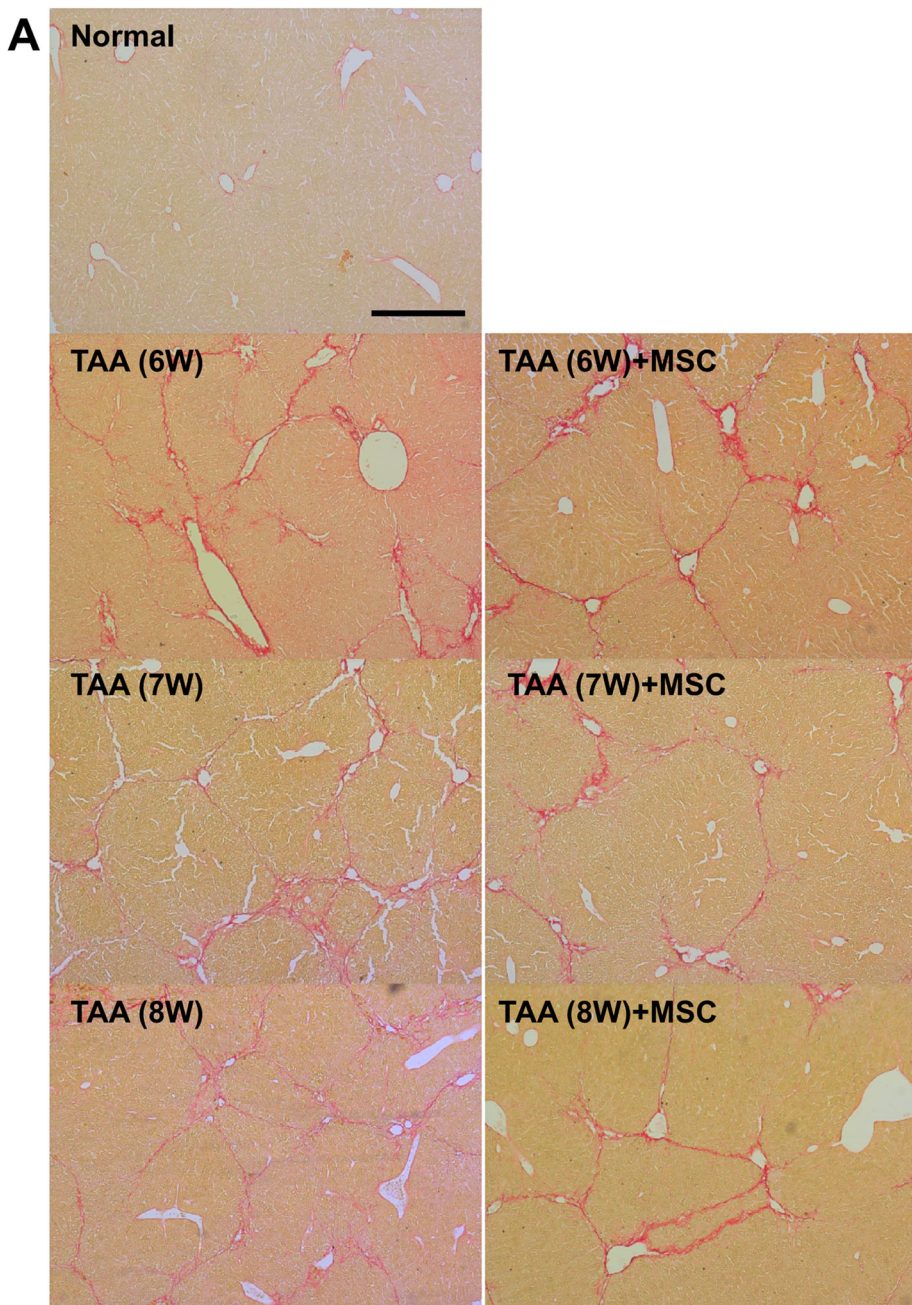
Fig. 1 Morphology and differentiation potential characterization of MSCs explanted from human Wharton's jelly tissues (WJ-MSCs) by incubation with differentiation inducing media, including adipogenesis, osteogenesis and chondrogenesis. **A** Morphology of fibroblast-like cells isolated by an explant method (passage 0, at day 5). **B** Expansion of mesenchymal stromal cells at passage 1 (day 10). **C** Flow cytometry showed WJ-MSCs at passage 2 expressing MSC phenotypic markers, including CD44, CD73, CD90, and CD105, but without expression of CD45/CD34/CD11b/CD19/HLA-DR surface antigens. **D** Adipogenesis of WJ-MSCs evidenced by Oil-red O stain.

Inset photo clearly shows oil droplets in adipocyte-like cells. **E** Induction of two adipocyte marker genes expression, peroxisome proliferator-activated receptor- γ (PPAR- γ) and glucose transporter type 4 (GLUT-4), was quantified by qPCR. **F** Osteogenesis of WJ-MSCs as shown by Alizarin red S staining. **G** Induction of two osteoblastic marker genes, osteopontin (OPN) and alkaline phosphatase (ALP). **H** Chondrogenesis of WJ-MSCs as shown by pellet formation. **I** Induction of two chondrocyte-specific genes, perlecan and syndecan. qPCR data are shown as mean \pm SD. * $p < 0.05$, versus time zero control

difference in hepatic FN mRNA levels between animals with and without WJ-MSC treatment (Supplemental Fig. S1), WJ-MSC administration significantly decreased hepatic pFN contents in the fibrotic livers after 2 weeks of

cell therapy (Fig. 3H). This finding strongly suggests a modulatory role of administered WJ-MSCs in hepatic pFN relocation and/or its stability.

Fig. 2 Amelioration of TAA-induced mouse liver fibrosis by intravenous administration with WJ-MSCs. **A** NOD-SCID mice received intraperitoneal TAA injection twice weekly for 6 weeks and received MSC infusion (3×10^5 cells per mouse) or PBS as vehicle control. After 3, 7, and 14 days of MSC therapy, liver tissues were collected for histopathological examination using Sirius red stain. Representative microphotographs showing typical fibrotic nodules and collagen deposition (red) in liver sections of TAA-treated mice. **B** Histomorphometrical analysis for percentage of collagen-deposited area showing reduction of intrahepatic collagen accumulation. Data are mean \pm SEM. $**p < 0.01$ and $***p < 0.001$, vs. vehicle control. NS, not significant. Scale bar, 200 μ m



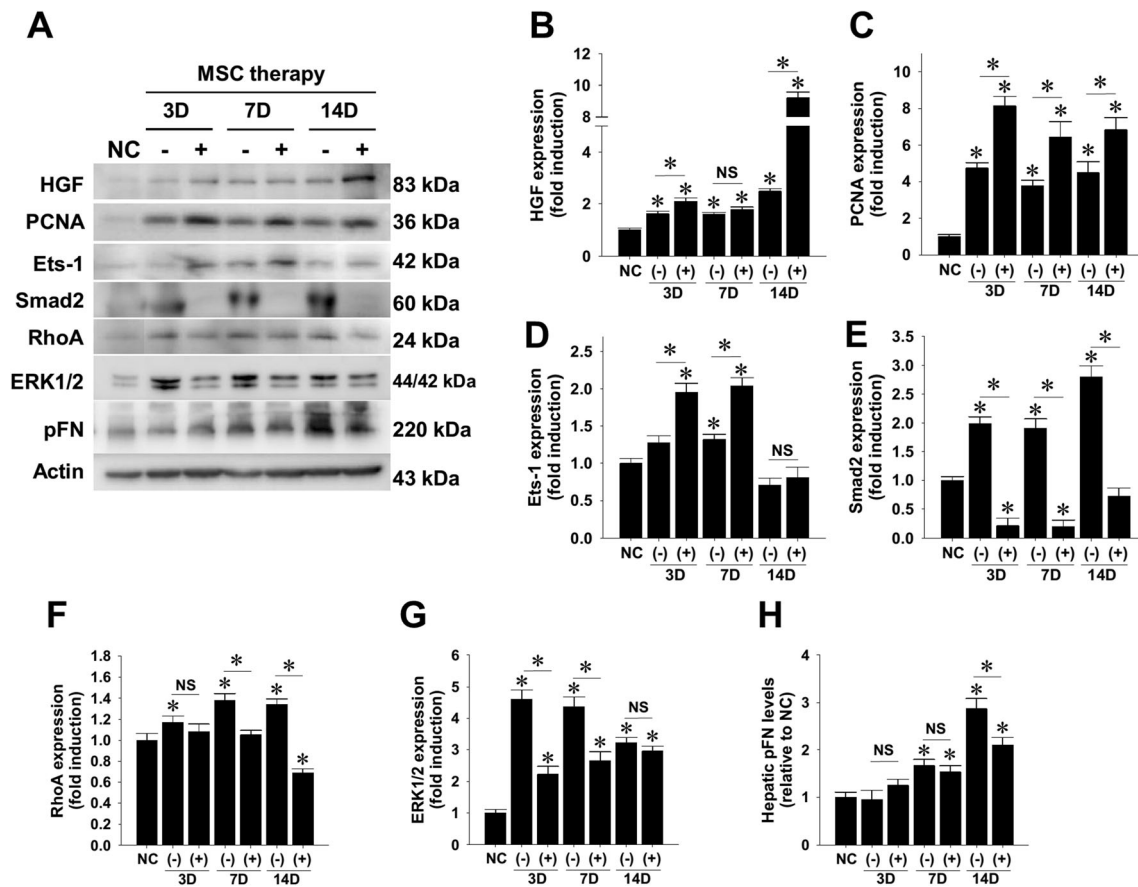


Fig. 3 Modulatory effects of WJ-MSC therapy on expression of regenerative and fibrotic markers in TAA-injured mouse livers. **A** NOD-SCID mice received intraperitoneal TAA injection twice weekly for 6 weeks and received MSC infusion (3×10^5 cells per mouse) or PBS as vehicle control. After 3, 7, and 14 days of WJ-MSC therapy, liver tissue and plasma proteins were collected for western

blotting detection. Relative expression levels of target proteins were subsequently measured by densitometry, including **B** HGF, **C** PCNA, **D** Ets-1 p42, **E** total Smad2, **F** RhoA, **G** ERK1/2, and **H** plasma fibronectin (pFN). Data are mean \pm SEM induction folds over control. * $p < 0.05$ compared with normal control (NC) or between indicated groups. NS, not significant

3.4 Modulation of pFN on adhesion and migration of WJ-MSCs

Despite the absence of fluorescent-labeled WJ-MSCs in the injured livers (data not shown), we suspected that the administered WJ-MSCs might activate the liver repairing machinery through modulating pFN functionality. To elucidate the mechanism underlying the reduction of hepatic pFN, we first explored whether pFN binds to circulating WJ-MSCs. However, flow cytometry revealed that pFN did not directly bind to the surface of suspending WJ-MSCs (Supplemental Fig. S2), ruling out the masking effect of pFN on suspending MSC via binding to surface integrins. Intriguingly, we noted that the suspended WJ-MSCs dramatically induced depolymerization and/or degradation of pFN in vitro (Fig. 4A). Meanwhile, WJ-MSCs were treated with soluble pFN and subject to cellular adhesion and migration assays. Adhesion assay results indicated that adhering ability of suspending WJ-MSCs to pFN-coated

dishes was significantly lower than that of the cells to type I collagen-coated dishes (Fig. 4B), while the suppressive effect appeared to be dose-dependent (Fig. 4C). Moreover, migration assay demonstrated that adherent WJ-MSCs grown on pFN-coated dishes exhibited higher migrating ability than those without ECM coating (Fig. 4D, E). These findings imply that the interaction between MSCs and pFN plays an important role in determining stem cell migratory ability.

3.5 Attenuation of TGF- β 1-induced pro-fibrogenic signal in activated HSCs by soluble pFN and WJ-MSC conditioned medium

Since MSC therapy is known to ameliorate pro-fibrogenic signals in experimental liver fibrosis models and cultured activated HSCs [22, 34–40], we next sought to investigate whether pFN and/or its MSC-conditioned medium would exhibit similar actions in a rat HSC cell line, HSC-T6 cells.

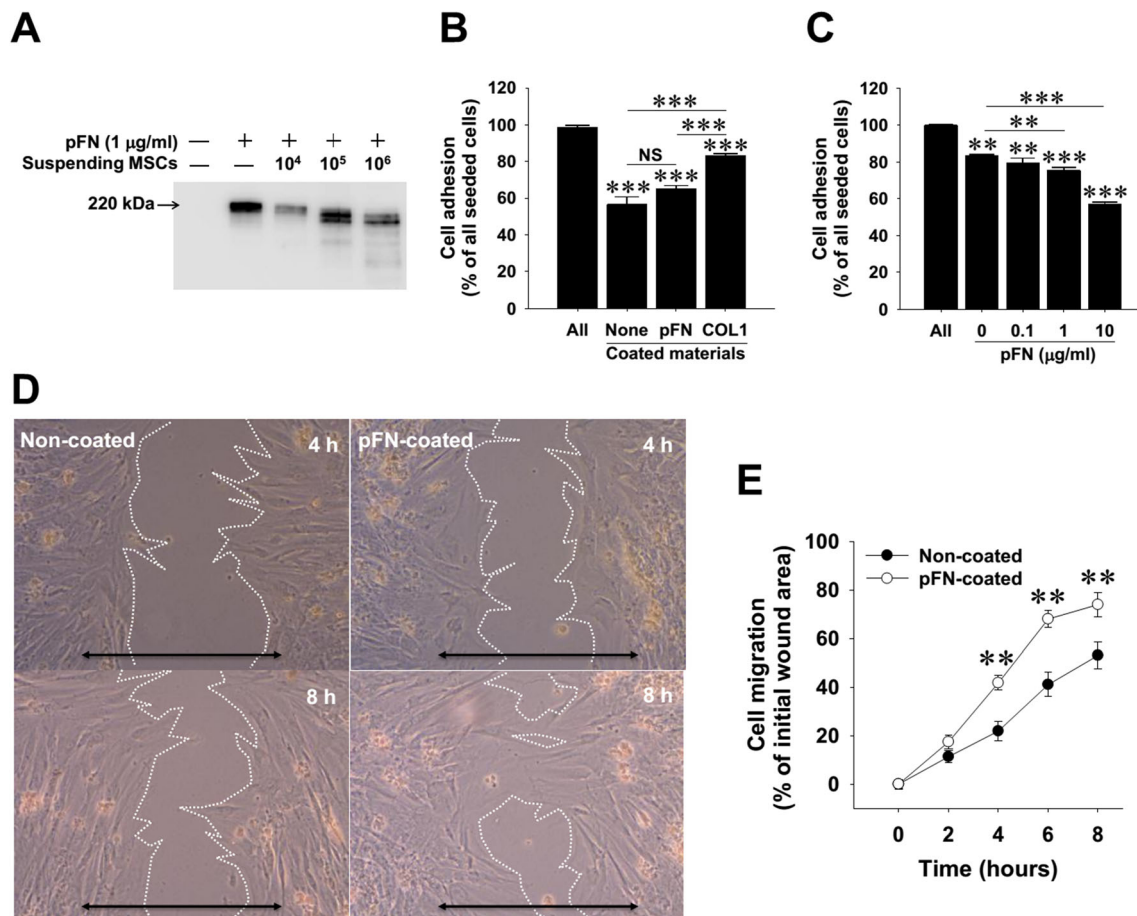


Fig. 4 Interactions between WJ-MSCs and plasma fibronectin (pFN) in vitro. **A** Western blotting detection on the serum-free conditioned media from suspending WJ-MSCs with or without pFN. **B** Adherence of suspending WJ-MSCs to surface precoated with different extracellular matrices. Cell adhering ability was determined by removing non-adherent cells 20 min after seeding. **C** Suppression of pFN on the binding ability of WJ-MSCs onto type I collagen (COL1)-coated

surface. **D** Representative images of wound-healing cell migration assay on WJ-MSC motility shot at 8 h. Double-headed arrow indicates initial wounded gap. Scale bars, 200 µm. **E** Quantitative data of wound-healing cell migration assay. All data are mean ± SD from three independent experiments. ** $p < 0.01$ and *** $p < 0.001$, vs. control, between indicated groups, non-coated control groups. NS, not significant

The effect on TGF-β1-elicited profibrogenic signals was first compared in the cells grown on non-coated and pFN-coated dishes (Fig. 5). Western blotting and subsequent densitometry clearly showed that pFN coating markedly enhanced TGF-β1-induced Smad2 hyperphosphorylation (Fig. 5D) and potentiated TGF-β1-upregulated RhoA protein expression (Fig. 5G), while pretreatment with soluble pFN partially ameliorated TGF-β1-stimulated Smad2 phosphorylation and dramatically abrogated RhoA upregulation in cells grown on pFN-coated dishes (Fig. 5B, E, H). Furthermore, pretreating conditioned medium of WJ-MSCs with soluble pFN completely inhibited TGF-β1-driven Smad2 phosphorylation as well as RhoA upregulation (Fig. 5C, F, I). These findings strongly support that WJ-MSCs, when combined with pFN, markedly suppress the profibrogenic signal from TGF-β1 stimulation.

4 Discussion

Although WJ-MSCs have been previously shown to effectively ameliorate chemically induced liver fibrosis in experimental rodent models [18, 19], the present study provides a novel molecular insight into the WJ-MSC therapeutics. FN is a multifunctional glycoprotein known to play a key role in governing fundamental cell behaviors, including embryogenesis, homeostasis, wound healing, and malignancy [41]. Notably, a major fraction of pFN present in tissue ECM has been found to be derived from plasma [42], highlighting the regulatory role of pFN in tissue homeostasis. One of the interesting findings of the present study was the significant reduction in pFN levels in the fibrotic murine livers after WJ-MSC therapy. Mechanistically, our results showed that WJ-MSCs could induce pFN degradation in vitro. Moreover, the conditioned medium

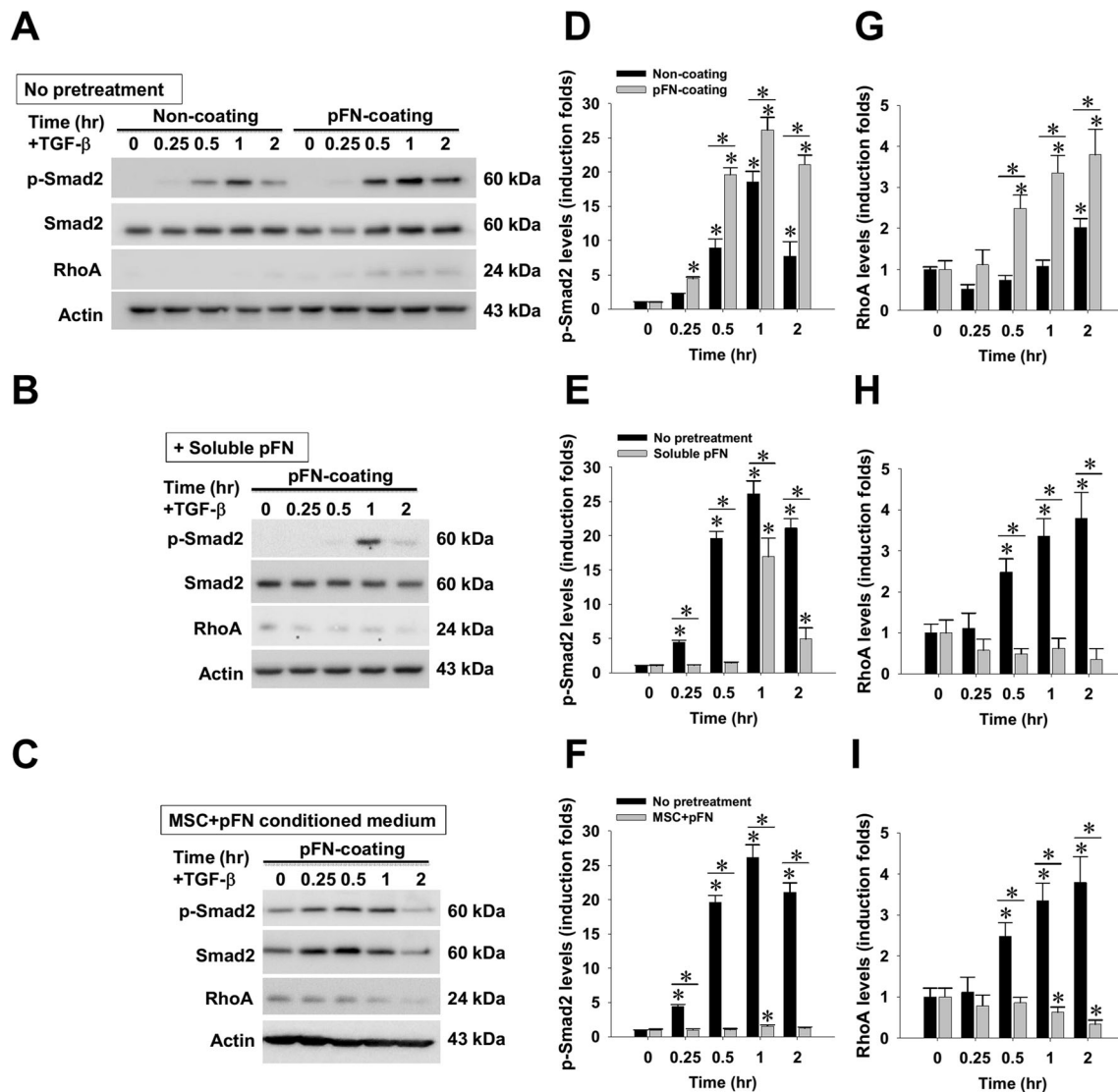


Fig. 5 Effects of soluble plasma fibronectin (pFN) and its WJ-MSC-conditioned media on the response of cultured HSC-T6 cells to TGF- β 1 stimulation. **A** HSC-T6 cells were grown on dishes pre-coated with or without pFN, received 2 h of serum starvation, followed by TGF- β stimulation (10 ng/ml). Alternatively, **B** soluble pFN or **C** serum-free conditioned media of WJ-MSCs with soluble pFN were added into

HSC-T6 cells 2 h before TGF- β stimulation. Western blotting and semi-quantitative densitometrical analysis were used to measure the contents of **D–F** cellular Smad2 phosphorylation and **G–I** RhoA protein. Density data are mean \pm SD from three independent experiments. * $p < 0.01$, vs. time zero control or between indicated groups

from WJ-MSCs and pFN effectively suppressed the TGF- β 1-driven profibrogenic signals. These observations strongly suggest that interactions between MSCs and pFN may have an important role to play in the effectiveness of MSCs against hepatic fibrogenesis.

Despite extensive discussion about the role of pFN in liver regeneration, no tangible link has been identified. Kwon et al. reported an immediate reduction in circulating pFN levels following hepatectomy in both human and rats as well as persistently low levels in those with cirrhosis. That study also demonstrated a correlation between pFN levels and the degree of liver regeneration in patients and the rats with TAA-induced cirrhosis [43]. Intriguingly,

administration of human pFN reportedly enhances liver regeneration and improves phagocytic function of the reticuloendothelial system in hepatectomized rats [44], while pFN supplementation in early phase reduces liver damage and improves rat survival from galactosamine-induced acute liver failure [45]. Although these findings support the pro-regenerative role of circulating pFN, little is known about the significance of hepatic pFN levels. Given that pFN may deposit in tissues [42, 46] and smaller FN fragments (180 kDa) lacking the ED-A domain is found to transiently appear in the regenerating liver after hepatectomy [47], our in vitro finding showing the pFN-degrading effect of WJ-MSCs may link to the reduction in

hepatic pFN deposition in the regenerating livers. It remains controversial that inhibition of endogenous fibronectin assembly and hepatic deposition may decrease collagen accumulation and improve liver function in experimental models of liver fibrosis [48]. Taken together, our findings showed that administration of WJ-MSCs may modulate the distribution of pFN between circulation and the liver. However, the detailed mechanism awaits further elucidation.

The beneficial effects of cellular therapy have been widely reported in rodent liver fibrosis models by using MSCs of different sources, including BM [22, 34, 36, 39], as well as adipose [49], amnion [35], and umbilical cord tissues [37]. It is well documented that MSC therapy may suppress TGF- β -driven profibrogenic signaling, including TGF- β receptor and Smad2/3 expression, and attenuate consequent HSC activation [34]. In agreement with our observation, umbilical cord-derived MSCs can ameliorate TAA-induced liver fibrosis in mice [37]. The present study showed, for the first time, that conditioned medium of WJ-MSCs and soluble pFN could effectively attenuate TGF-driven Smad2 phosphorylation and RhoA upregulation in cultured HSC-T6 cells. The finding was consistent with the previously reported MSC-related paracrine effect in which soluble factors secreted from MSCs were found to decrease hepatic macrophage infiltration and modulate HSC activation [38]. Moreover, the secretomes derived from umbilical cords in particular is evidenced to attenuate TGF- β signaling machinery in TAA-treated mouse livers [37]. Also, previous studies have demonstrated that conditioned medium as well as extracellular vesicles from cultured MSCs ameliorate CCl₄-induced hepatic inflammation and attenuate HSC activation in rodents [24, 35]. Although our findings are consistent with those of previous studies, it is still noteworthy that treatment with MSC conditioned medium may elevate the constitutive levels of Smad2 phosphorylation and RhoA expression in the HSC-T6 cells grown on pFN-coated dishes. Even though this elevation might contribute to enhanced collagen deposition in the fibrotic liver shortly after WJ-MSC administration (i.e., 3 days) and result in the blunted response of cultured HSCs to TGF- β stimulation (Fig. 2B), we cannot rule out the possibility that WJ-MSC therapy might have short-term deleterious effects on the signaling machinery in resident liver cells.

As a vital player in the TGF- β signaling axis, RhoA protein can deliver Smad-dependent or -independent signals for HSC activation [50]. In the regenerative niche of muscle fibers, a Wnt4-Rho signaling axis is recently found to constrain satellite cell numbers and their activation, while RhoA disruption is essential for muscle stem cell activation [51]. In the setting of liver fibrosis, the present study provides the first evidence that WJ-MSC therapy

reduces hepatic RhoA expression in fibrotic livers and its conditioned medium with pFN further abrogates TGF- β 1-induced RhoA upregulation. In line with our observation, the conditioned medium from BM-derived MSCs is previously demonstrated to decrease RhoA expression in HSCs and retards their proliferation via regulation of cell cycle regulator P27 [36]. Our findings may shed additional light on the molecular mechanism underlying WJ-MSC therapy.

The present study had several limitations. Firstly, the use of xenotransplantation inevitably limits its clinical applicability. Secondly, because of the lack of functional lymphocytes in immunodeficient NOD-SCID mice, we did not evaluate the effect of lymphocyte depletion on hepatic pFN expression and its dynamic tissue relocation under pathologic conditions. Because the adherence of infiltrating lymphocytes to hepatic FN is known to contribute to the pathogenesis of liver cirrhosis [52], the role of lymphocyte could not be elucidated with this animal model. Thirdly, introduction of WJ-MSCs into the systemic circulation via the venous system instead of direct administration into the hepatic artery may diminish the therapeutic effectiveness because of possible sequestration of MSCs in the lungs [53] rather than the injured liver. On the other hand, MSCs residing in the lungs may still secrete soluble factors or extracellular microvesicles that enhance liver regeneration [35, 37]. Furthermore, the use of hepatotoxins to create a liver fibrosis animal model may damage other non-liver organs. Indeed, a TAA dose equivalent to that used in this study has been reported to cause proximal renal tubular injuries [54]. Therefore, the possibility of hepatic regeneration signals from other injured organs remains to be elucidated.

In conclusion, this study demonstrated that WJ-MSC therapy ameliorated TAA-induced chronic liver injury and exerted pFN-lowering effect in mice. In addition, *in vitro* mechanistic study showed that conditioned medium of WJ-MSCs with soluble pFN effectively attenuated TGF-driven Smad2 phosphorylation and RhoA upregulation in cultured HSCs. These findings highlight the significance of hepatic pFN and MSC-derived soluble factors in the regeneration process of hepatic fibrogenesis.

Acknowledgements The authors would like to dedicate this article to late Professor Daniel Tzu-Bi Shih in memory of his earnestness and generosity in disseminating his knowledge and sharing his expertise with his fellow researchers. This study was supported by the Grants from E-Da Hospital (EDAHP102043 to CYC; NCKUEDA10513 to YHK; EDAHT107047 to CKS). YHK, CYC and CKS conceived the study, supervised the experiments and finalized the draft. YHK and YCL wrote the paper. YCL, CWL and PHC performed the experiments. PHL, TST, YCC, and MHC contributed to analysis tools and analyzed the data. All authors have reviewed the manuscript and approved submission.

YHK, CYC and CKS conceived the study, supervised the experiments and finalized the draft. YHK and YCL wrote the paper. YCL, CWL and PHC performed the experiments. PHL, TST, YCC, and MHC contributed to analysis tools and analyzed the data. All authors have reviewed the manuscript and approved submission.

Compliance with ethical standards

Conflict of interest The authors declare that they have no conflict of interest.

Ethical statement The study protocol was approved by the institutional reviewing board of E-Da Hospital (IRB No. EMRP26100N). Informed consent was confirmed by the IRB. The animal studies were performed after receiving approval of the Institutional Animal Care and Use Committee at E-Da Hospital (IACUC Approval No. IACUC-101017).

References

- Bissell DM. Hepatic fibrosis as wound repair: a progress report. *J Gastroenterol.* 1998;33:295–302.
- Tsukada S, Parsons CJ, Rippe RA. Mechanisms of liver fibrosis. *Clin Chim Acta.* 2006;364:33–60.
- Friedman SL. Molecular mechanisms of hepatic fibrosis and principles of therapy. *J Gastroenterol.* 1997;32:424–30.
- Qian J, Niu M, Zhai X, Zhou Q, Zhou Y. β -Catenin pathway is required for TGF- β inhibition of PPARG γ expression in cultured hepatic stellate cells. *Pharmacol Res.* 2012;66:219–25.
- Deng X, Deng L, Wang P, Cheng C, Xu K. Post-translational modification of CREB-1 decreases collagen I expression by inhibiting the TGF- β 1 signaling pathway in rat hepatic stellate cells. *Mol Med Rep.* 2016;14:5751–9.
- Okita K, Yamanaka S. Induction of pluripotency by defined factors. *Exp Cell Res.* 2010;316:2565–70.
- McElreavey KD, Irvine AI, Ennis KT, McLean WH. Isolation, culture and characterisation of fibroblast-like cells derived from the Wharton's jelly portion of human umbilical cord. *Biochem Soc Trans.* 1991;19:29S.
- Takechi K, Kuwabara Y, Mizuno M. Ultrastructural and immunohistochemical studies of Wharton's jelly umbilical cord cells. *Placenta.* 1993;14:235–45.
- Kobayashi K, Kubota T, Aso T. Study on myofibroblast differentiation in the stromal cells of Wharton's jelly: expression and localization of alpha-smooth muscle actin. *Early Hum Dev.* 1998;51:223–33.
- Wang HS, Hung SC, Peng ST, Huang CC, Wei HM, Guo YJ, et al. Mesenchymal stem cells in the Wharton's jelly of the human umbilical cord. *Stem Cells.* 2004;22:1330–7.
- Fong CY, Chak LL, Biswas A, Tan JH, Gauthaman K, Chan WK, et al. Human Wharton's jelly stem cells have unique transcriptome profiles compared to human embryonic stem cells and other mesenchymal stem cells. *Stem Cell Rev Rep.* 2011;7:1–16.
- Mitchell KE, Weiss ML, Mitchell BM, Martin P, Davis D, Morales L, et al. Matrix cells from Wharton's jelly form neurons and glia. *Stem Cells.* 2003;21:50–60.
- Chao KC, Chao KF, Fu YS, Liu SH. Islet-like clusters derived from mesenchymal stem cells in Wharton's Jelly of the human umbilical cord for transplantation to control type 1 diabetes. *PLoS One.* 2008;3:e1451.
- Conconi MT, Burra P, Di Liddo R, Calore C, Turetta M, Bellini S, et al. CD105(+) cells from Wharton's jelly show in vitro and in vivo myogenic differentiative potential. *Int J Mol Med.* 2006;18:1089–96.
- Wu KH, Zhou B, Lu SH, Feng B, Yang SG, Du WT, et al. In vitro and in vivo differentiation of human umbilical cord derived stem cells into endothelial cells. *J Cell Biochem.* 2007;100:608–16.
- Zhang YN, Lie PC, Wei X. Differentiation of mesenchymal stromal cells derived from umbilical cord Wharton's jelly into hepatocyte-like cells. *Cytotherapy.* 2009;11:548–58.
- Anzalone R, Lo Iacono M, Corrao S, Magno F, Loria T, Cappello F, et al. New emerging potentials for human Wharton's jelly mesenchymal stem cells: immunological features and hepatocyte-like differentiative capacity. *Stem Cells Dev.* 2010;19:423–38.
- Tsai PC, Fu TW, Chen YM, Ko TL, Chen TH, Shih YH, et al. The therapeutic potential of human umbilical mesenchymal stem cells from Wharton's jelly in the treatment of rat liver fibrosis. *Liver Transpl.* 2009;15:484–95.
- Lin SZ, Chang YJ, Liu JW, Chang LF, Sun LY, Li YS, et al. Transplantation of human Wharton's Jelly-derived stem cells alleviates chemically induced liver fibrosis in rats. *Cell Transplant.* 2010;19:1451–63.
- Sakaida I, Terai S, Yamamoto N, Aoyama K, Ishikawa T, Nishina H, et al. Transplantation of bone marrow cells reduces CCl4-induced liver fibrosis in mice. *Hepatology.* 2004;40:1304–11.
- Higashiyama R, Inagaki Y, Hong YY, Kushida M, Nakao S, Niioka M, et al. Bone marrow-derived cells express matrix metalloproteinases and contribute to regression of liver fibrosis in mice. *Hepatology.* 2007;45:213–22.
- Sun CK, Chen CH, Kao YH, Yuen CM, Sheu JJ, Lee FY, et al. Bone marrow cells reduce fibrogenesis and enhance regeneration in fibrotic rat liver. *J Surg Res.* 2011;169:e15–26.
- Sáez-Lara MJ, Frecha C, Martín F, Abadía F, Toscano M, Gil A, et al. Transplantation of human CD34+ stem cells from umbilical cord blood to rats with thioacetamide-induced liver cirrhosis. *Xenotransplantation.* 2006;13:529–35.
- Kim YH, Cho KA, Park M, Kim HS, Park JW, Woo SY, et al. Conditioned medium from tonsil-derived mesenchymal stem cells relieves CCl4-induced liver fibrosis in mice. *Tissue Eng Regen Med.* 2019;16:51–8.
- De Bruyn C, Najjar M, Raicevic G, Meuleman N, Pieters K, Stamatopoulos B, et al. A rapid, simple, and reproducible method for the isolation of mesenchymal stromal cells from Wharton's jelly without enzymatic treatment. *Stem Cells Dev.* 2011;20:547–57.
- Chang CY, Chen PH, Li CJ, Lu SC, Lin YC, Lee PH, et al. Isolation and characterization of mesenchymal stem cells derived from human umbilical cord blood mononuclear cells. *E-Da Medical Journal.* 2016;3:1–13.
- Kao YH, Chen CL, Jawan B, Chung YH, Sun CK, Kuo SM, et al. Upregulation of hepatoma-derived growth factor is involved in murine hepatic fibrogenesis. *J Hepatol.* 2010;52:96–105.
- Junqueira LC, Bignolas G, Brentani RR. Picrosirius staining plus polarization microscopy, a specific method for collagen detection in tissue sections. *Histochem J.* 1979;11:447–55.
- Goodman ZD, Becker RL Jr, Pockros PJ, Afdhal NH. Progression of fibrosis in advanced chronic hepatitis C: evaluation by morphometric image analysis. *Hepatology.* 2007;45:886–94.
- Chang YC, Kao YH, Hu DN, Tsai LY, Wu WC. All-trans retinoic acid remodels extracellular matrix and suppresses laminin-enhanced contractility of cultured human retinal pigment epithelial cells. *Exp Eye Res.* 2009;88:900–9.
- Wu WC, Lai YH, Hsieh MC, Chang YC, Wu MH, Wu HJ, et al. Pleiotropic role of atorvastatin in regulation of human retinal pigment epithelial cell behaviors in vitro. *Exp Eye Res.* 2011;93:842–51.

32. Kao YH, Chen PH, Wu TY, Lin YC, Tsai MS, Lee PH, et al. Lipopolysaccharides induce Smad2 phosphorylation through PI3K/Akt and MAPK cascades in HSC-T6 hepatic stellate cells. *Life Sci.* 2017;184:37–46.
33. Jiang Y, Xu W, Lu J, He F, Yang X. Invasiveness of hepatocellular carcinoma cell lines: contribution of hepatocyte growth factor, c-met, and transcription factor Ets-1. *Biochem Biophys Res Commun.* 2001;286:1123–30.
34. Sun XE, Zhang XQ, Liu MM. Effect of bone marrow mesenchymal stem cells on the TGF- β 1/Smad signaling pathway of hepatic stellate. *Genet Mol Res.* 2015;14:8744–54.
35. Ohara M, Ohnishi S, Hosono H, Yamamoto K, Yuyama K, Nakamura H, et al. Extracellular vesicles from amnion-derived mesenchymal stem cells ameliorate hepatic inflammation and fibrosis in rats. *Stem Cells Int.* 2018;2018:3212643.
36. Qin S, Jiang H, Su S, Wang D, Liang Z, Zhang J, et al. Inhibition of hepatic stellate cell proliferation by bone marrow mesenchymal stem cells via regulation of the cell cycle in rat. *Exp Ther Med.* 2012;4:375–80.
37. An SY, Jang YJ, Lim HJ, Han J, Lee J, Lee G, et al. Milk fat globule-EGF factor 8, secreted by mesenchymal stem cells, protects against liver fibrosis in mice. *Gastroenterology.* 2017;152:1174–86.
38. Huang B, Cheng X, Wang H, Huang W, la Ga HuZ, Wang D, et al. Mesenchymal stem cells and their secreted molecules predominantly ameliorate fulminant hepatic failure and chronic liver fibrosis in mice respectively. *J Transl Med.* 2016;14:45.
39. Qiao H, Zhou Y, Qin X, Cheng J, He Y, Jiang Y. NADPH oxidase signaling pathway mediates mesenchymal stem cell-induced inhibition of hepatic stellate cell activation. *Stem Cells Int.* 2018;2018:1239143.
40. Wang J, Sun M, Liu W, Li Y, Li M. Stem cell-based therapies for liver diseases: an overview and update. *Tissue Eng Regen Med.* 2019;16:107–18.
41. To WS, Midwood KS. Plasma and cellular fibronectin: distinct and independent functions during tissue repair. *Fibrogenesis Tissue Repair.* 2011;4:21.
42. Moretti FA, Chauhan AK, Iaconcig A, Porro F, Baralle FE, Muro AF. A major fraction of fibronectin present in the extracellular matrix of tissues is plasma-derived. *J Biol Chem.* 2007;282:28057–62.
43. Kwon AH, Inada Y, Uetsuji S, Yamamura M, Hioki K, Yamamoto M. Response of fibronectin to liver regeneration after hepatectomy. *Hepatology.* 1990;11:593–8.
44. Kwon AH, Uetsuji S, Yamamura M, Hioki K, Yamamoto M. Effect of administration of fibronectin or aprotinin on liver regeneration after experimental hepatectomy. *Ann Surg.* 1990;211:295–300.
45. Moriyama T, Aoyama H, Ohnishi S, Imawari M. Protective effects of fibronectin in galactosamine-induced liver failure in rats. *Hepatology.* 1986;6:1334–9.
46. Oh E, Pierschbacher M, Ruoslahti E. Deposition of plasma fibronectin in tissues. *Proc Natl Acad Sci U S A.* 1981;78:3218–21.
47. Pujades C, Forsberg E, Enrich C, Johansson S. Changes in cell surface expression of fibronectin and fibronectin receptor during liver regeneration. *J Cell Sci.* 1992;102:815–20.
48. Altrock E, Sens C, Wuerfel C, Vasel M, Kawelke N, Dooley S, et al. Inhibition of fibronectin deposition improves experimental liver fibrosis. *J Hepatol.* 2015;62:625–33.
49. De Luna-Saldivar MM, Marino-Martinez IA, Franco-Molina MA, Rivera-Morales LG, Alarcón-Galván G, Cordero-Pérez P, et al. Advantages of adipose tissue stem cells over CD34(+) mobilization to decrease hepatic fibrosis in Wistar rats. *Ann Hepatol.* 2019;18:620–6.
50. Cho JJ, Kim YW, Han CY, Kim EH, Anderson RA, Lee YS, et al. E-cadherin antagonizes transforming growth factor beta1 gene induction in hepatic stellate cells by inhibiting RhoA-dependent Smad3 phosphorylation. *Hepatology.* 2010;52:2053–64.
51. Eliazar S, Muncie JM, Christensen J, Sun X, D'Urso RS, Weaver VM, et al. Wnt4 from the niche controls the mechano-properties and quiescent state of muscle stem cells. *Cell Stem Cell.* 2019;25:654–65.e4.
52. Bruck R, Hershkoviz R, Lider O, Aeed H, Zaidel L, Matas Z, et al. Inhibition of experimentally-induced liver cirrhosis in rats by a nonpeptidic mimetic of the extracellular matrix-associated Arg–Gly–Asp epitope. *J Hepatol.* 1996;24:731–8.
53. Hayes-Jordan A, Wang YX, Walker P, Cox CS. Mesenchymal stromal cell dependent regression of pulmonary metastasis from Ewing's. *Front Pediatr.* 2014;2:44.
54. Barker EA, Smuckler EA. Nonhepatic thioacetamide injury. II. The morphologic features of proximal renal tubular injury. *Am J Pathol.* 1974;74:575–90.

Publisher's Note Springer Nature remains neutral with regard to jurisdictional claims in published maps and institutional affiliations.